

BRIEF NOTE • OPEN ACCESS

GaN growth on ScAlMgO₄ substrates via thermally-dewetted thin Al films

To cite this article: Alessandro Floriduz and Elison Matioli 2022 *Jpn. J. Appl. Phys.* **61** 118003

View the [article online](#) for updates and enhancements.

You may also like

- [High quality nitride semiconductors grown on novel ScAlMgO₄ substrates and their light emitting diodes](#)
Akio Ueta, Hiroshi Ohno, Naoto Yanagita et al.
- [High-temperature thermal expansion of ScAlMgO₄ for substrate application of GaN and ZnO epitaxial growth](#)
Rayko Simura, Kazumasa Sugiyama, Akihiko Nakatsuka et al.
- [Ab initio calculations on the initial stages of GaN and ZnO growth on lattice-matched ScAlMgO₄ \(0001\) substrates](#)
Yao Guo, Yanfei Wang, Chengbo Li et al.



GaN growth on ScAlMgO₄ substrates via thermally-dewetted thin Al films

Alessandro Floriduz* and Elison Matioli*

Power and Wide-Band-Gap Electronics Research Laboratory, Institute of Electrical and Micro Engineering, École Polytechnique Fédérale de Lausanne, 1015 Lausanne, Switzerland

*E-mail: alessandro.floriduz@epfl.ch; elison.matioli@epfl.ch

Received August 2, 2022; revised September 11, 2022; accepted October 5, 2022; published online October 31, 2022

In this note, we demonstrate the high-temperature growth of GaN on ScAlMgO₄ substrates by metalorganic vapor phase epitaxy when a thin Al film is deposited ex situ on the ScAlMgO₄ surface, prior to GaN growth. Mirror-like high-quality GaN epitaxial layers were obtained when N₂ was used as carrier gas during the reactor temperature ramp-up preceding GaN growth, leading to a higher GaN quality compared to direct growth on ScAlMgO₄ using a trimethylaluminium preflow. This opens a pathway for high-temperature GaN growth on ScAlMgO₄ when an Al precursor line is not present. © 2022 The Author(s). Published on behalf of The Japan Society of Applied Physics by IOP Publishing Ltd

Supplementary material for this article is available [online](#)

ScAlMgO₄ (SAM) has recently emerged as an attractive alternative to conventional substrates for GaN heteroepitaxy, thanks to its minimal mismatch in *a*-lattice constant and coefficient of thermal expansion with respect to GaN.^{1–6} Successful growth of GaN on SAM by metalorganic vapor phase epitaxy (MOVPE) was first demonstrated by using low-temperature (LT) GaN buffers,^{6–9} analogously to growth on sapphire. Recently, we demonstrated the direct high-temperature (HT) growth of GaN on SAM without LT buffers by means of a trimethylaluminium (TMAI) preflow.¹⁰ In this note, we investigate the growth of GaN on SAM by MOVPE without LT GaN buffers using a thin Al film deposited ex situ (e.g. by electron-beam evaporation) on the SAM surface prior to GaN growth, as an alternative to in situ TMAI preflow (both methods aiming to cover the SAM surface with Al atoms). Here we demonstrate that such an approach for growth of GaN on SAM is not only feasible, but also leads to a higher GaN quality compared to the use of an in situ TMAI preflow. In particular, we show that the aluminium films deposited ex situ on SAM substrates thermally dewet during the reactor temperature ramp-up, forming Al islands that may be responsible for the improved GaN quality by promoting an initial 3D growth of GaN at HT. Moreover, the proposed technique does not require a reactor bake-out before growth. The presented method would enable the HT growth of GaN on SAM when the TMAI line is not present. In addition, this approach might also be extended for the growth of SAM by halide vapor phase epitaxy (HVPE), for which the presence of an Al source boat poses constraints on the reactor design and operation,¹¹ thus hampering the possibility of an in situ preflow.

All experiments were performed on 0.5 mm-thick *c*-plane SAM chips of size 9 mm × 10 mm, with top-side polished, provided by Fukuda Crystal Laboratory.¹ Each chip was cleaned in acetone, isopropanol and deionized water for 10 min and then loaded into an electron-beam evaporator for the deposition of a thin Al film on the SAM surface (base pressure = 2×10^{-7} mbar, Al target purity = 99.99%, deposition rate = 1 \AA s^{-1}). After that, the samples were loaded into a showerhead MOVPE reactor (AIXTRON CCS $3 \times 2''$) for GaN growth within 20 min after the end of the evaporation, during which time the samples were exposed to air. GaN

growth was monitored in situ with a reflectance measurement system.

As a first experiment, we performed GaN growth on a SAM sample with an Al film of a thickness (t_{Al}) of 5 nm evaporated on its surface. The growth recipe started with reactor heating from room temperature up to 1065 °C, with H₂ as the carrier gas; then, the NH₃ line was opened (with a flow of 22 mmol min^{-1}) for a 3 min long nitridation at 1065 °C. Subsequently, the NH₃ flow was ramped to $134 \text{ mmol min}^{-1}$ and the temperature was decreased to 1020 °C in 2 min. After that, the trimethylgallium (TMGa) line was opened to start GaN growth. The TMGa flow was $115 \text{ \mu mol min}^{-1}$ (V/III ratio = 1165), leading to a GaN growth rate of 2.2 \mu m h^{-1} . Unless otherwise stated, the GaN layer thickness was fixed at 1.3 \mu m . Throughout the whole recipe, the reactor pressure was 200 mbar and H₂ was used as a carrier gas.

Under these conditions and with $t_{\text{Al}} = 5 \text{ nm}$, the grown GaN surface was very rough [Fig. 1(a)]. The reflectance signal [Fig. 1(b)] provides insightful information to understand the growth dynamics: the initial reflectance is high due to the Al film covering the SAM surface; then, during the temperature ramp-up, at around 600 °C the reflectance sharply drops to a value close to that of a pristine polished SAM surface. After that, it does not vary significantly until the start of GaN growth. We attribute this steep change in reflectance to thermal dewetting^{12,13} of the evaporated Al film on SAM, leading to the formation of Al islands. Then, at the opening of the TMGa line, the reflectance starts increasing due to GaN growth [Fig. 1(b)]; the signal presents oscillations, although very damped, indicating high roughness of the GaN surface [evident from Fig. 1(a)]. The GaN layer was N-polar, as determined by etching in KOH solution (7 mol l^{-1}) at 60 °C for 10 min.

To verify that Al film dewetting actually occurred, we loaded another SAM sample with a 5 nm-thick Al film into the MOVPE reactor and interrupted the growth recipe during the initial temperature ramp-up at 850 °C, before any GaN layer was grown. Figures 1(c) and 1(d) show the bright-field and corresponding dark-field optical images of the sample surface after unloading from the reactor: the Al film evidently agglomerated into islands, hence confirming the dewetting



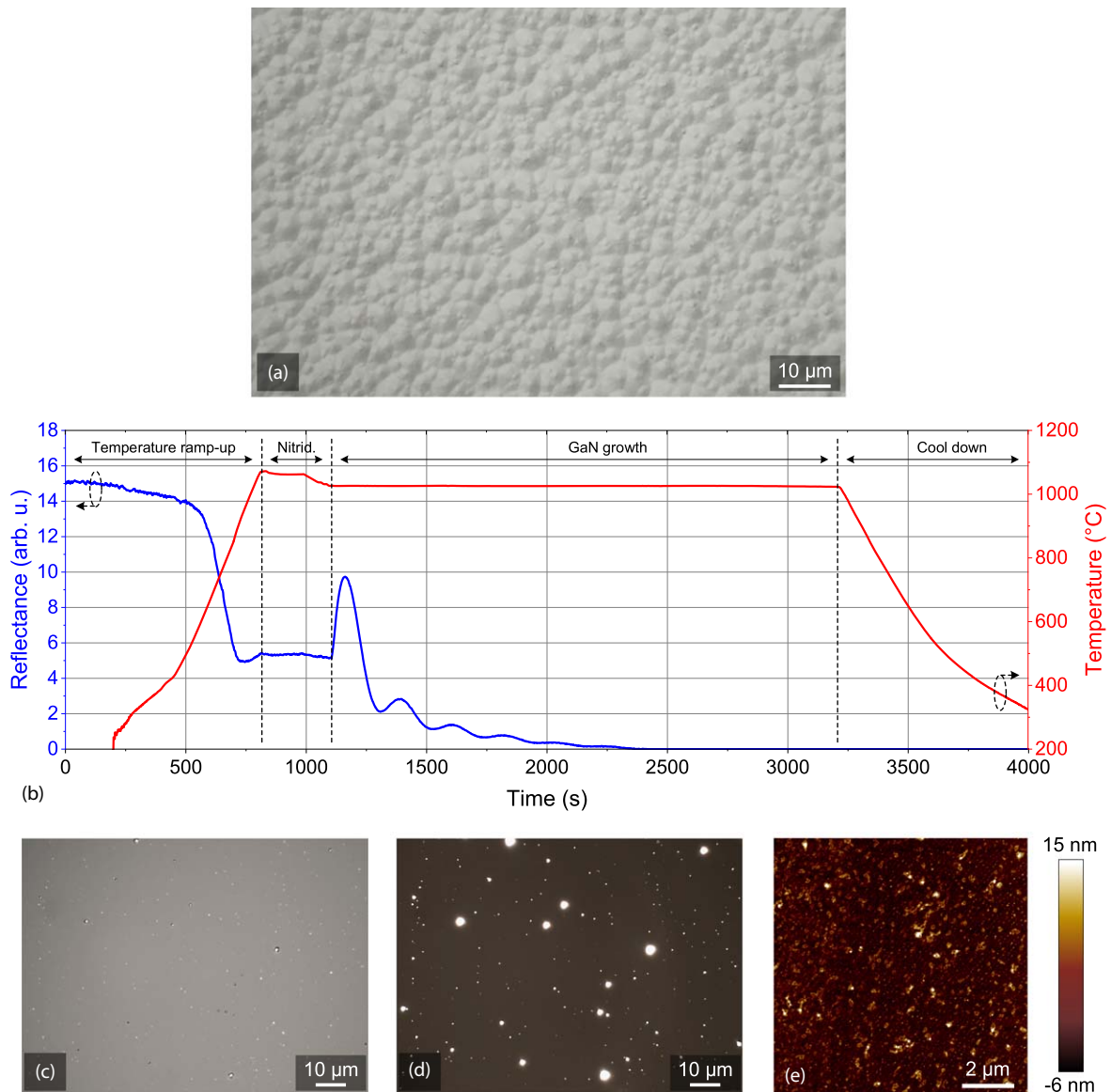


Fig. 1. (Color online) (a) Nomarski image of the surface of GaN grown on a SAM sample with $t_{Al} = 5$ nm and H_2 as a carrier gas during dewetting. (b) Reflectance diagram and measured temperature during growth for the sample in (a). (c) Optical bright-field, (d) dark-field, and (e) AFM images of the SAM surface for a sample with $t_{Al} = 5$ nm after recipe interruption during temperature ramp-up at 850 °C under H_2 .

mechanism. The sample presented an average RMS surface roughness from atomic force microscopy (AFM) measurements of 4.7 nm [Fig. 1(e)], much smaller than the laser wavelength of the reflectance system (635 nm): this explains why after dewetting, the reflectance drops to virtually the same value as a pristine SAM surface.

Aiming to improve the GaN crystallinity, we evaluated the use of N_2 instead of H_2 as the carrier gas during dewetting, since the quality of the GaN epilayer should depend on the dewetting process of the Al film itself. All parameters and conditions were the same as before, except that N_2 was initially used as a carrier gas instead of H_2 ; the carrier gas was then switched back to H_2 after nitridation at 1065 °C and before the start of GaN growth. On the samples with a 5 nm-thick Al film on SAM, this growth was successful and a uniform crack-free Ga-polar GaN film with a mirror-like surface was obtained, as shown in Fig. 2(a). The AFM measurements showed that the GaN surface exhibited the typical step-and-terrace structure [Figs. 2(b)–2(c)], confirming the good morphological quality of the sample. The

reflectance diagram [Fig. 2(d)] presented major differences compared to the previous case [Fig. 1(b)]. First, Al dewetting occurred at a higher temperature than under H_2 (~700 °C). Then, at the start of GaN growth, reflectance oscillations immediately began and reached full amplitude within 4 cycles, clearly indicating an improved GaN morphology compared to dewetting under H_2 .

To understand better the dewetting process under N_2 , we loaded into the MOVPE reactor another SAM sample with $t_{Al} = 5$ nm and interrupted the growth recipe during the initial temperature ramp-up at 850 °C. Compared to dewetting under H_2 [Figs. 1(c)–1(e)], a much higher density of Al islands was found for the same t_{Al} , as shown by Figs. 2(e)–2(g); this also resulted in a larger RMS surface roughness of 16.7 nm. We may attribute these differences in dewetting with N_2 to the following reasons: (i) the surface tension for Al is influenced by the gas environment and is different for H_2 and N_2 ;¹⁴⁾ (ii) H_2 can detach the native oxide¹⁵⁾ covering the top of the evaporated Al film (which naturally forms within few minutes of air exposure,¹⁶⁾ before loading into the

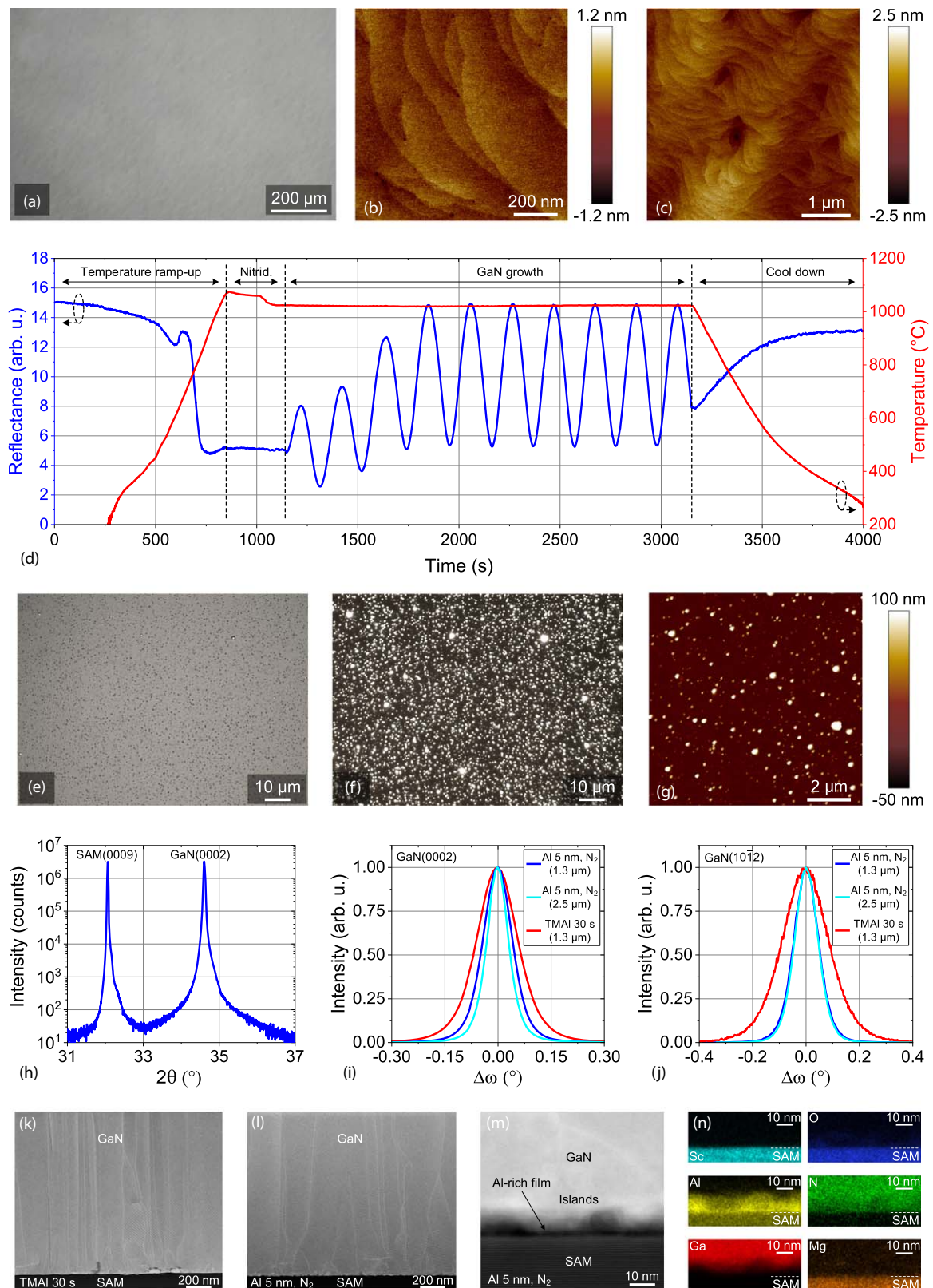


Fig. 2. (Color online) (a) Nomarski image of the surface of GaN grown on a SAM sample with $t_{Al} = 5$ nm and N_2 as a carrier gas during dewetting. (b)–(c) AFM images of the GaN surface after growth relative to the sample in (a). (d) Reflectance diagram and measured temperature during growth for the sample in (a). (e) Optical bright-field, (f) dark-field, and (g) AFM images of the SAM surface for a sample with $t_{Al} = 5$ nm after recipe interruption during temperature ramp-up at 850 °C under N_2 . (h) Symmetric 2θ - ω XRD scan of the same GaN sample in (a). Normalized X-ray rocking curves for (i) GaN(0002) and (j) GaN(10 $\bar{1}$ 2) reflections for GaN samples (with a thickness of 1.3 and 2.5 μ m) grown on SAM with $t_{Al} = 5$ nm and N_2 during dewetting and for a GaN sample (with a thickness of 1.3 μ m) directly grown on SAM using a TMAI preflow of 30 s. HAADF STEM images of the 1.3 μ m-thick GaN samples on SAM grown with (k) a TMAI preflow of 30 s and (l)–(m) with $t_{Al} = 5$ nm and N_2 during dewetting. (n) STEM EDX of (m) indicating almost continuous Al coverage at the SAM surface.

MOVPE reactor), which also plays a role during dewetting.¹³⁾

Figure 2(h) illustrates the X-ray diffraction (XRD) 2θ - ω scan of the same GaN-on-SAM sample of Figs. 2(a)–2(d), where only two peaks are visible, corresponding to SAM(0009) and GaN(0002). The X-ray rocking curves (XRCs) for the GaN(0002) and GaN(10 $\bar{1}$ 2) reflections [Figs. 2(i)–2(j)] reveal FWHM values of 350 and 393 arcsec, respectively, for a GaN thickness of only 1.3 μ m. The crystalline quality further improved in a sample grown in the same way having a GaN thickness of 2.5 μ m, which presented FWHM values of 259 and 372 arcsec for the GaN(0002) and GaN(10 $\bar{1}$ 2) XRC peaks, respectively [Figs. 2(i)–2(j)]. These values appear to be promising when compared to previous reports on GaN-on-SAM layers with LT buffers.^{6–9)} More importantly, the proposed technique led to a higher crystalline quality compared to direct HT growth on SAM with TMAI preflow: In comparison, a GaN layer (with the same GaN growth conditions and thickness of 1.3 μ m) was grown on a pristine SAM sample, using a TMAI preflow of 30 s as in Ref. 10, and exhibited XRCs with FWHM values of 491 and 740 arcsec for the (0002) and (10 $\bar{1}$ 2) peaks, respectively [Figs. 2(i)–2(j)]. This clearly indicates that a lower threading dislocation density (TDD) is achieved when the Al film is deposited ex situ compared to use of a TMAI preflow. A lower TDD was also observed from high-angle annular dark-field (HAADF) scanning transmission electron microscopy (STEM) images [Figs. 2(k)–2(l)], which also showed a stronger interaction between threading dislocations for the sample with evaporated Al film. Therefore, we may attribute such decrease in TDD to a difference in growth mode: with TMAI preflow, the growth starts directly in 2D mode;¹⁰⁾ conversely, with an evaporated Al film, GaN growth presents an initial 3D mode (evident from the reflectance signal) induced by the Al islands, which can promote threading dislocation, bending and annihilation, analogously to GaN growth on sapphire with LT GaN buffer or epitaxial lateral overgrowth.¹⁷⁾

As a possible mechanism for GaN growth on SAM after Al dewetting, we speculate that Al islands are not completely disconnected immediately after dewetting, but rather connected by an ultra-thin (few monolayer-thick) Al film covering the SAM surface. Similar to dewetting of Cu on Ta;¹²⁾ we may also speculate that such ultra-thin layer is more easily attacked by H₂ than N₂. From our previous results, direct HT growth of GaN on a pristine or nitridated SAM surface results in N-polarity, while Ga-polarity is obtained when SAM is covered by an Al layer.¹⁰⁾ Therefore, for dewetting under H₂, we suppose that with $t_{Al} = 5$ nm the ultra-thin Al layer disappears before TMGa opening, so that GaN grows directly on SAM, resulting in N-polarity; for thicker t_{Al} (e.g. $t_{Al} = 10$ nm and $t_{Al} = 15$ nm, see Fig. S1 of the supplementary data), the ultra-thin film may still cover part of the SAM surface at TMGa opening, so that GaN grows on such film (leading to Ga-polarity) but resulting in a poor morphology with many uncoalesced regions (due to incomplete coverage). For dewetting under N₂, the ultra-thin film may still cover most of the SAM surface (even with only $t_{Al} = 5$ nm), therefore leading to a uniform Ga-polar film. STEM images (including energy dispersive X-ray mapping) of the GaN/SAM interface for $t_{Al} = 5$ nm and dewetting

under N₂ confirm the presence of an almost continuous Al-rich layer (presumably AlN) on the SAM surface [Figs. 2(m)–2(n)], thus supporting our hypothesis. A more detailed investigation of Al dewetting on SAM and the GaN nucleation mechanism will be subject of further works.

Finally, we conclude that, unlike growth on SAM with TMAI preflow,¹⁰⁾ the proposed method does not require a reactor bake-out (i.e. thermal cleaning in H₂) ahead of loading the sample for GaN epitaxy, thus speeding up the growth procedure even considering the ex situ Al evaporation. This might be because the Al film is already present on the SAM surface before reactor heating, and hence might be less influenced by the decomposition of GaN residues inside the reactor which could alter the SAM surface during temperature ramp-up.

In conclusion, we demonstrated that GaN can be grown at HT on SAM by MOVPE when a thin Al layer is evaporated on the SAM substrate prior to GaN epitaxy. When N₂ was used as a carrier gas during the initial reactor temperature ramp-up, we obtained a mirror-like GaN layers exhibiting a significant improvement in crystalline quality compared to the direct growth on SAM with a TMAI preflow. Moreover, the proposed method may also be extended to GaN growth on SAM by HVPE, eliminating the need for an initial GaN template by MOVPE and thus simplifying the realization of free-standing GaN layers.

Acknowledgments The authors gratefully thank Damien Trolliet, Yoan Trolliet, Nicolas Leiser, Dr. Jean-François Carlin (EPFL) for technical support, and Dr. Victor Boureau and Dr. Lucie Navratilova (CIME, EPFL) for STEM imaging. This work was supported in part by the Swiss National Science Foundation (SNSF) under the project number 200021_200652.

ORCID iDs Alessandro Floriduz  <https://orcid.org/0000-0003-2795-2135> Elisa Matioli  <https://orcid.org/0000-0001-6475-001X>

- 1) T. Fukuda, Y. Shiraishi, T. Nanto, T. Fujii, K. Sugiyama, R. Simura, H. Iechi, and K. Tadamoto, *J. Cryst. Growth* **574**, 126286 (2021).
- 2) R. Simura, K. Sugiyama, A. Nakatsuka, and T. Fukuda, *Jpn. J. Appl. Phys.* **54**, 075503 (2015).
- 3) M. Velazquez-Rizo, M. Najmi, D. Iida, P. Kirilenko, and K. Ohkawa, *Appl. Phys. Express* **15**, 065501 (2022).
- 4) R. Takahashi, R. Fujiki, K. Hozo, R. Hiramatsu, M. Matsukura, T. Kojima, D.-P. Han, M. Iwaya, T. Takeuchi, and S. Kamiyama, *Appl. Phys. Lett.* **120**, 142102 (2022).
- 5) T. Ozaki, M. Funato, and Y. Kawakami, *Appl. Phys. Express* **8**, 062101 (2015).
- 6) T. Ozaki, Y. Takagi, J. Nishinaka, M. Funato, and Y. Kawakami, *Appl. Phys. Express* **7**, 091001 (2014).
- 7) T. Iwabuchi, S. Kuboya, T. Tanikawa, T. Hanada, R. Katayama, T. Fukuda, and T. Matsuoka, *Phys. Status Solidi A* **214**, 1600754 (2017).
- 8) A. Ueta, H. Ohno, N. Yanagita, N. Ryoki, K. Miyano, A. Ishibashi, and M. Nobuoka, *Jpn. J. Appl. Phys.* **58**, SC1041 (2019).
- 9) T. Fukui, T. Sakaguchi, Y. Matsuda, M. Matsukura, T. Kojima, M. Funato, and Y. Kawakami, *Jpn. J. Appl. Phys.* **61**, 090904 (2022).
- 10) A. Floriduz and E. Matioli, *Jpn. J. Appl. Phys.* **61**, 048002 (2022).
- 11) T. Yamane, F. Satoh, H. Murakami, Y. Kumagai, and A. Koukitu, *J. Cryst. Growth* **300**, 164 (2007).
- 12) F. Fillot, Z. Tokei, and G. P. Beyer, *Surf. Sci.* **601**, 986 (2007).
- 13) S. W. Hieke, B. Breitbach, G. Dehm, and C. Scheu, *Acta Mater.* **133**, 356 (2017).
- 14) R. Saravanan, J. Molina, J. Narciso, C. Garcia-Cordovilla, and E. Louis, *J. Mater. Sci. Lett.* **21**, 309 (2002).
- 15) M. Li, D.-G. Xie, E. Ma, X.-X. Zhang, and Z.-W. Shan, *Nat. Commun.* **8**, 14564 (2017).
- 16) N. Cai, G. Zhou, K. Mueller, and D. Starr, *Phys. Rev. B* **84**, 125445 (2011).
- 17) P. Vennéguès, B. Beaumont, V. Bousquet, M. Vaille, and P. Gibart, *J. Appl. Phys.* **87**, 4175 (2000).